

On Periodically Pendulum-Driven Systems for Underactuated Locomotion: a Viscoelastic Jointed Model

Pengcheng Liu¹ (PhD student), *Student Member, IEEE*, Hongnian Yu¹ and Shuang Cang²

¹ *Faculty of Science and Technology, Bournemouth University, Poole BH125BB, UK*

² *Faculty of Management, Bournemouth University, Poole BH125BB, UK*

Abstract—This paper investigates the locomotion principles and nonlinear dynamics of the periodically pendulum-driven (PD) systems using the case of a 2-DOF viscoelastic jointed model. As a mechanical system with underactuation degree one, the proposed system has strongly coupled nonlinearities and can be utilized as a potential benchmark for studying complicated PD systems. By mathematical modeling and non-dimensionalization of the physical system, an insight is obtained to the global system dynamics. The proposed 2-DOF viscoelastic jointed model establishes a commendable interconnection between the system dynamics and the periodically actuated force. Subsequently, the periodic locomotion principles of the actuated subsystem are elaborately studied and synthesized with the characteristic of viscoelastic element. Then the qualitative changes are conducted respectively under the varying excitation amplitude and frequency. Simulation results validate the efficiency and performance of the proposed system comparing with the conventional system.

Keywords-pendulum-driven systems; periodic motion; underactuated ; viscoelasticity

I. INTRODUCTION

Applications of underactuated mechanical systems (UMSs) have been penetrated into extensive branches of technology in the domain of robotics and control communities. These systems excel in performing complicated tasks with a reduced number of actuators, which imply an increased manoeuvrability, optimized energy consumptions as well as reduced cost.

Starting with these viewpoints, the motions with a repeated pattern at periodically intervals raise interests for various applications, for instance, the walking or running of the creatures, which under a regular pattern in their implementation. This attracts significant devotions to the trajectory planning and nonlinear control of UMSs by the robotics and control communities during the past few decades. The researchers are addressing both the theoretical difficulties [1]–[3] and the practical challenges [4]–[6]. Among these researches, the UMSs employing a pendulum or a system of the pendulums, which is referred to as PD UMSs, permits the investigations on selecting different important nonlinear effects. Attentions have been paid to the classical pendulum UMSs, as benchmarks, including the Acrobot [7]–[9], the Pendubot [10]–[12], the cart-pole system [13], the crane systems [14], [15], Furuta pendulum systems [16], [17]. Besides, numerous applications of such systems are known in engineering, for

instance, in vibro-absorption problems [18], [19], in trajectory tracking control of PD systems [20]–[22]. However, making a stabilized periodic motion trajectory (limit cycle) through feedback laws has been proved to be essential for nonlinear control.

The employment of viscoelastic property in the applications of UMSs has many advantages. For instance, higher bandwidth mechanical compliance, larger working space, better manoeuvrability, higher convergence rate and lower energy consumption are regarded as important indexes to evaluate the performance of the robot systems. Viscoelasticity has been studied extensively in the past two decades, including impact force reduction [23], trajectory planning [24], nonlinearities analysis such as hysteresis and friction [25], dynamic and static stability [26], etc. However, challenges are still remained in trajectory planning and controller design for the UMSs in the presence of strong coupled nonlinear dynamics, i.e., how to govern the dynamics for the underactuated locomotion.

This paper investigates the periodic locomotion principles in the case of a 2-DOF PD system, which has potential applications such as pipeline inspection, medical assistance and information acquisition in disaster rescues. The aim of this paper is to shed light on the aforementioned nontrivial challenges by calling attentions to the issue of periodic motion trajectory synthesis and nonlinear dynamic analysis through numerical investigations of the characteristics of the proposed system.

The rest of the paper is organized as follows. Section II describes the formulation of the problem. Periodic locomotion principles synthesis is provided in Section III. Section IV investigates the system nonlinearities, and analyses the periodic and chaotic behaviours under varying excitation amplitude and frequency. Simulation results are presented in Section V. Finally, conclusions are given in Section VI.

II. PROBLEM FORMULATION

This study considers the nonlinear viscoelastic model shown in Fig.1, which consists of an inverted pendulum coupled with a 2-DOF spring-mass-damper system and is subjected to a periodical actuation applied at the pivot. The masses, spring and the dashpot in the 2-DOF system

are all identical and the locomotion of the proposed system is in horizontal plane.

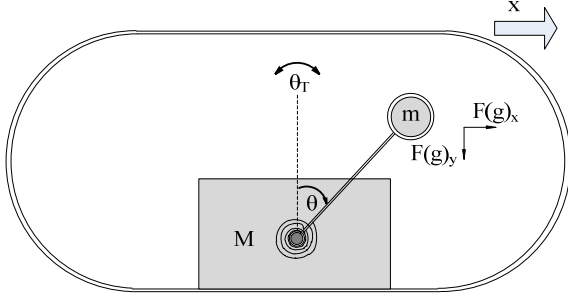


Figure 1. The 2-DOF spring-mass-damper system coupled with a nonlinear pendulum

It is assumed that mass of the pendulum rod is omitted and the centre of mass of the rotating mechanism is coinciding with the centre of the ball which is fixed rigidly at the end of the pendulum. Furthermore, the air frictional resistance is supposed to be zero when the pendulum is rotating. The torsional spring is un-stretched when the inverted pendulum is upright. M and m are the masses of the base and the ball, respectively. l is the length of the inverted pendulum, θ and x depict the configuration variables of the rotational and the horizontal movements, i.e. $q = [q_1 \ q_2]^T = [\theta \ x]^T$, k and c represent the stiffness and damping coefficients, respectively. It is also assumed that the configuration variables θ and x are measured from the equilibrium position of the inverted pendulum and the original point of the base.

Employing the Coulomb friction model to describe the resistance force between the proposed PD locomotive system and the environmental surface, gives

$$f = \begin{cases} 0, & \dot{x} = 0 \\ \mu F(g)_y \text{sgn}(\dot{x}), & \dot{x} \neq 0 \end{cases} \quad (1)$$

where μ is the Coulomb friction coefficient, $F(g)_y$ represents the force applied on the platform in the vertical direction.

Based on the aforementioned assumptions and definitions, the equations of motion governing the dynamic behaviour the proposed model can be derived using the Euler-Lagrangian approach

$$\frac{d}{dt} \frac{\partial L(q_i, \dot{q}_i)}{\partial \dot{q}_i} - \frac{\partial L(q_i, \dot{q}_i)}{\partial q_i} + \frac{\partial D(\dot{q}_i)}{\partial \dot{q}_i} = Bu + Q_\zeta \quad (2)$$

where $L(q_i, \dot{q}_i)$ reflects the difference between the kinetic energy $E(q_i, \dot{q}_i)$ and the potential energy $V(q_i)$, $D(\dot{q}_i)$ describes the dissipative energy. $B \in IR^{n \times n}$ is a constant matrix, u is the control input, Q_ζ represents the effects of uncertainties and disturbances.

The developed dynamic equations of motion are

$$ml^2\ddot{\theta} - ml\cos\theta\ddot{x} - mgl\sin\theta + k\theta + c\dot{\theta} = \theta_T \quad (3)$$

$$\begin{aligned} -ml[\cos\theta + \mu\sin\theta\text{sgn}(\dot{x})]\ddot{\theta} + (M+m)\ddot{x} + ml[\sin\theta \\ - \mu\cos\theta\text{sgn}(\dot{x})]\dot{\theta}^2 + \mu[(M+m)g \\ - (k\theta + c\dot{\theta})\sin\theta/l]\text{sgn}(\dot{x}) = 0 \end{aligned} \quad (4)$$

where θ_T is the rotational controlled torque applied to the inverted pendulum.

Our goal is to create periodic progression of the proposed system via an elaborate design of the rotational trajectory of the inverted pendulum and an appropriate feedback action. Consequently, the following desired periodic function and its derivative are adopted

$$\theta_T = -A\cos(\Omega t), \quad \dot{\theta}_T = A\Omega\sin(\Omega t) \quad (5)$$

where A and Ω are respectively the amplitude and frequency of the periodic excitation.

We further define the following non-dimensional parameters

$$\begin{aligned} \tau = \omega_n t, \quad X = \frac{x}{l}, \quad \omega_n = \sqrt{\frac{g}{l}}, \quad \omega = \frac{\Omega}{\omega_n}, \\ \lambda = \frac{M}{m}, \quad \rho = \frac{k}{ml^2\omega_n^2}, \quad \nu = \frac{c}{ml^2\omega_n}, \quad h = \frac{A}{ml^2\omega_n^2} \end{aligned} \quad (6)$$

Adopting the desired periodic function and the parameters above, Eq. (3) and Eq. (4) reduce to the following non-dimensional form

$$[\mathcal{M}]\{\xi\}'' + [\mathcal{C}]\{\xi\}' + [\mathcal{N}]\{\xi\} + [\mathcal{Q}] = \{\mathcal{U}\} \quad (7)$$

where

$$[\mathcal{M}] = \begin{bmatrix} 1 & -\cos\theta \\ -[\cos\theta + \mu\sin\theta\text{sgn}(\dot{X})] & (\lambda + 1) \end{bmatrix},$$

$$[\mathcal{C}] = \begin{bmatrix} \nu \\ [\sin\theta - \mu\cos\theta\text{sgn}(\dot{X})]\dot{\theta} - \mu\nu\sin\theta\text{sgn}(\dot{X}) \end{bmatrix},$$

$$[\mathcal{N}] = \rho\hat{\alpha} \begin{bmatrix} 1 \\ -\sin\theta \end{bmatrix},$$

$$[\mathcal{Q}] = \hat{\alpha} \begin{bmatrix} 0 \\ (\lambda + 1) - (\rho h \cos\omega\tau - \nu h \omega \sin\omega\tau)\sin\theta \end{bmatrix},$$

$$\{\mathcal{U}\} = \begin{bmatrix} -\rho h \cos\omega\tau + \nu h \omega \sin\omega\tau \\ 0 \end{bmatrix}, \quad \hat{\alpha} = \mu\text{sgn}(\dot{X}),$$

and the aforementioned derivations are operated with respect to the dimensionless time τ and the configuration variables in the dimensionless time coordinate become

$$\{\xi\} = \begin{Bmatrix} \xi_1 \\ \xi_2 \end{Bmatrix} = \begin{Bmatrix} \theta \\ X \end{Bmatrix}.$$

Remark 1: In essence, the proposed PD locomotive system is a 2-DOF mechanical system with underactuation degree one. The underactuated nature results in the unavailability in the direct control of the locomotion of the platform. Furthermore, notwithstanding the fact that the proposed system is simple in structure, strong coupling and high nonlinearity exist in the dynamics which are originated from the trigonometric functions and the signal function. It is important to note that the sliding friction in the horizontal direction plays a vital role in the locomotion of the platform. This motivates the authors to scrutinize the characteristics of the periodic rotational torque and precisely design the locomotion principles for the actuated θ -subsystem.

III. PERIODIC LOCOMOTION PRINCIPLES SYNTHESIS

In this section, the periodic locomotion principles are generated for synthesizing the rotational motion of the inverted pendulum and the harmonic property of the viscoelastic element. It is considered that the nontrivial characteristic of viscoelastic element is equivalent to the existence of the periodic trajectory manifold with homologous arguments.

To effectively utilize the rotational motion of the pendulum and optimally drive the proposed 2-DOF system moving forward, the viscoelastic property is considered to synthesize the different periodic motions between the dissipated pendulum and the torsional spring, thus synthesized periodic locomotion principle is developed. In particular, three stages below are defined to generate the desired periodic locomotion.

- Initialization stage ($\tau = 0$) and re-initialization stage ($\tau = \tau_7$) (Fig. 3): one cycle of progressive motion begins and ends respectively with the initialization and re-initialization stages. In initialization stage, the pendulum and the torsional spring are constrained and kept stationary at a predesigned negative angle to the opposite direction of the retraction of spring, which stores potential energy in such a manner that more mechanical power is injected into the whole system; at the end of the motion, the pendulum gradually returns to the initial position by following the motion profile (to be described below), the system then is reinitialized with stored elastic energy.
- Progressive stage ($\tau \in (0, \tau_3)$): the torque motor drives the pendulum fast in the forward direction, together with the energy-releasing of the torsional spring, leads the system to overcome the maximal dry friction and therefore, a continuous progression of the whole system is obtained;
- Restoring stage ($\tau \in (\tau_4, \tau_7)$): the pendulum gradually returns to the initial position since the resultant force in the horizontal direction is less than the maximal dry friction, that is, the whole system is kept stationary in this stage of duration.

In view of the aforementioned locomotion principles, the desired periodic motion trajectory profiles of the dissipated pendulum and the torsional spring are presented in Fig.2, respectively.

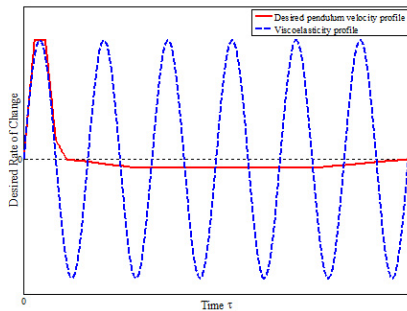


Figure 2. Synthesis of the periodic motion trajectory profiles

It is worth mentioning that the net progression during one full motion cycle occurs in the progressive stage, in which the synthesis procedure is mainly carried out. Moreover, as one of the key elements regarding to the progression of the whole system, the friction between the platform and the sliding surface is taken into account for designing the restoring stage through the consideration of the system constraints. Therefore, the synthesized periodic locomotion profile generated using Eq. (8) is shown in Fig. 3, wherein the zoom up window demonstrates the detailed profile in the progressive stage.

$$\dot{\theta}_{Td} = \begin{cases} P_1 \omega \sin(\omega \tau), & \tau \in [0, \tau_1) \\ P_1 \omega, & \tau \in [\tau_1, \tau_2) \\ P_1 \omega \sin(\omega \tau - \tau_2), & \tau \in [\tau_2, \tau_3) \\ \frac{\tau_3 - \tau}{\tau_3 - \tau_2} P_2, & \tau \in [\tau_3, \tau_4) \\ \frac{\tau_4 - \tau}{\tau_4 - \tau_3} P_3, & \tau \in [\tau_4, \tau_5) \\ -P_3, & \tau \in [\tau_5, \tau_6) \\ \frac{\tau_6 - \tau}{\tau_6 - \tau_5} P_3, & \tau \in [\tau_6, \tau_7) \end{cases} \quad (8)$$

where P_1 and P_2 respectively describe the upper and lower boundary of the trajectory, P_3 is the critical boundary when the system begins to keep stationary, ω is frequency of periodic excitation.

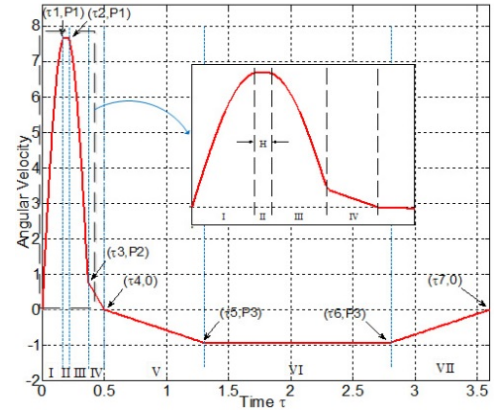


Figure 3. Synthesized periodic locomotion profile for one full cycle

The explicit description of the periodic locomotion principles are as follows:

- Initialization

$$\tau = 0 : \theta(\tau) = \theta_{min} = -\theta_0, X(\tau) = 0, \dot{\theta}(\tau) = 0, \dot{X}(\tau) = 0, \ddot{\theta}(\tau) = 0, \ddot{X}(\tau) = 0$$

The pendulum together with the torsional spring is kept stationary at a predesigned negative angle $-\theta_0$ to the opposite direction of the retraction of spring, which stores potential energy such that more mechanical power will be injected into the system.

- Phase I

$$\tau \in (0, \tau_1) : \theta(\tau) = \theta > 0, X(\tau) = x, \dot{\theta}(\tau) > 0, \dot{X}(\tau) > 0, \ddot{\theta}(\tau) \gg 0, \ddot{X}(\tau) > 0$$

The torque motor begins to move under the synthesized angular velocity and simultaneously the stored potential energy is released from the

stretched torsional spring. This results in a motion with maximal angular acceleration of the pendulum pushing the base moving forward with acceleration;

- Phase II

$$\tau \in [\tau_1, \tau_2) : \theta(\tau) = \theta > 0, X(\tau) = x, \dot{\theta}(\tau) > 0, \dot{X}(\tau) > 0, \ddot{\theta}(\tau) = 0, \ddot{X}(\tau) > 0$$

It is noted that once the potential energy is released, a short period of time is required to let the potential energy fully transfer into kinetic energy of the proposed system. This leads to a more efficient energy consumption. Thus a short period of uniform motion of the pendulum is designed. During this period, the pendulum swings forward with the maximal angular velocity while driving the base accelerating continuously;

- Phase III

$$\tau \in [\tau_2, \tau_3) : \theta(\tau) = \theta > 0, X(\tau) = x, \dot{\theta}(\tau) > 0, \dot{X}(\tau) > 0, \ddot{\theta}(\tau) < 0, \ddot{X}(\tau) < 0$$

The torque actuation exerts an opposing force on the pendulum under the synthesized angular velocity together with the contractility of the torsional spring. This leads to a forward deceleration motion of the pendulum as well as the base;

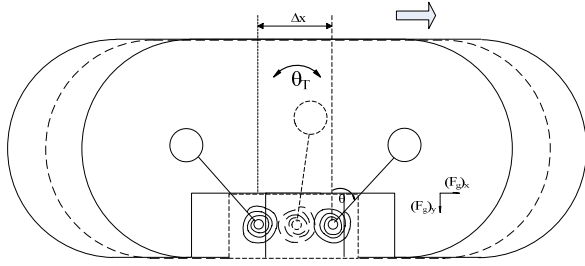


Figure 4. Locomotion of the 2-DOF pendulum-driven system in progressive stage

- Phase IV

$$\tau \in [\tau_3, \tau_4) : \theta(\tau) = \theta_{max} > 0, X(\tau) = x \rightarrow 0, \dot{\theta}(\tau) \rightarrow 0, \dot{X}(\tau) = 0, \ddot{\theta}(\tau) < 0, \ddot{X}(\tau) = 0$$

In phase IV, a slow deceleration motion of the pendulum results in the stationary of the base, which is subjected to the constraints under the dissipative force lie in the sliding surface as well as the pivot. Moreover, the angular displacement of the pendulum is constrained at θ_{max} to avoid over-actuation and system failure.

- Phase V

$$\tau \in [\tau_4, \tau_5) : \theta(\tau) = \theta < 0, X(\tau) = x, \dot{\theta}(\tau) < 0, \dot{X}(\tau) = 0, \ddot{\theta}(\tau) < 0, \ddot{X}(\tau) = 0$$

Phase V is designed to be a short duration and to generate a relatively low angular acceleration of the pendulum which keeps the base stands still;

- Phase VI

$$\tau \in [\tau_5, \tau_6) : \theta(\tau) = \theta < 0, X(\tau) = a\Delta x, \dot{\theta}(\tau) = -P_3 < 0, \dot{X}(\tau) = 0, \ddot{\theta}(\tau) = 0, \ddot{X}(\tau) = 0$$

A uniform angular velocity of the pendulum is designed for the purpose of gradually stretching the torsional spring such that enough potential energy is restored for the next cycle. The base remains stationary in this phase. $a\Delta x$ represents the net displacement of the base after the a^{th} cycle.

- Phase VII

$$\tau \in [\tau_6, \tau_7) : \theta(\tau) = \theta < 0, X(\tau) = a\Delta x, -P_3 < \dot{\theta}(\tau) < 0, \dot{X}(\tau) = 0, \ddot{\theta}(\tau) > 0, \ddot{X}(\tau) = 0$$

In phase VII, a low angular deceleration motion is generated in a short duration to decelerate the pendulum while the base keeps stationary;

- Re-Initialization

$$\tau = 0 : \theta(\tau) = \theta_{min} = -\theta_0, X(\tau) = a\Delta x, \dot{\theta}(\tau) = 0, \dot{X}(\tau) = 0, \ddot{\theta}(\tau) = 0, \ddot{X}(\tau) = 0$$

When the pendulum reaches to the initial angle, the torsional spring is constrained to θ_{min} such that enough elastic energy is stored for the next cycle.

Remark 2: The proposed periodic locomotion principles can be utilized for generating a class of appropriate trajectory profiles for PD underactuated mechanical systems with viscoelastic elements. The trajectory synthesis occurred at the progressive stage is the main enhancement comparing with the work in [27]. To obtain an optimal progression of the proposed system for one full motion cycle and to avoid unpredictable chaotic motions, it is necessary to find the optimal amplitude and frequency of the periodic force.

IV. NONLINEAR DYNAMIC ANALYSIS

Due to the fact that the proposed system is analytically unsolvable, a sequence of solutions is numerically calculated using the first order Euler algorithm in Matlab. In this section, we employ a visual interpretation on the dynamic behaviour affected respectively by the amplitude and frequency of the periodic force, and the stability variance of solutions accompanied by the varying values.

A. Qualitative Analysis of Amplitude h

The bifurcation diagram in Fig. 5 presents a projection of the Poincaré map on the dimensionless configuration axis. It clearly illustrates the richness of the system dynamics along with various transitions in the system response. It is noted that a large region of period-one response can be observed for $h \in [0.15, 1.174]$. Accompanied by increasing the excitation amplitude, a large window of chaotic motion is depicted for h in $(1.174, 2.1]$.

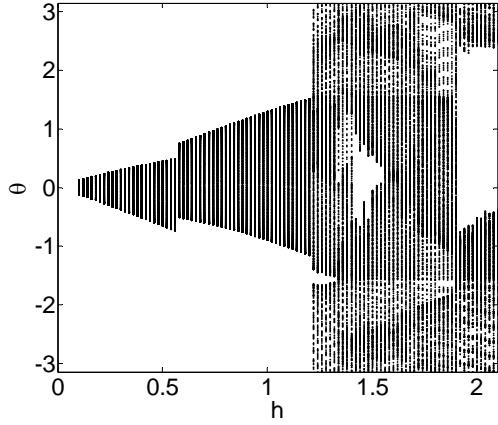


Figure 5. Bifurcation diagram of average progression of the 2-DOF PD system under varying excitation amplitude

Fig. 6 describes the trajectories on the dimensionless time coordinate, presenting the angular displacement of the inverted pendulum computed for various amplitudes of excitations. The characteristic of the irregular transitions under varying excitation amplitude, behaves atypical responses. These originate from the complicated interactions between different coexisting periodic orbits and bifurcations. The time histories of the angular displacement are important to appreciate the behaviours illustrated. At relatively low amplitude of excitation as shown in Figs. 6 (a) and (b), the pendulum employs simple but steady oscillation after the initial transients have decayed, which would repeat continuously. On the other hand, the motions contained in Figs. 6 (c) and (d) become chaotic at relatively high amplitude of excitation, which are extremely complex nonrepeating functions of time.

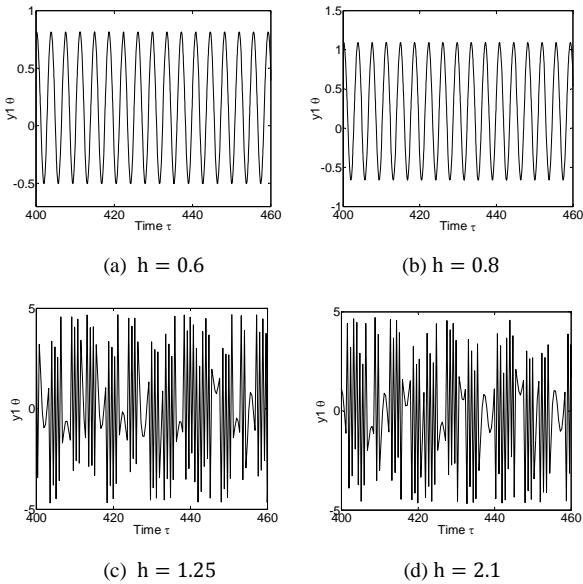


Figure 6. The time histories of the angular displacement of the inverted pendulum on dimensionless time coordinate

B. Qualitative Analysis of Frequency ω

The parameter dependence on varying frequency ω is studied as the second branching parameter and clearly

shown as a bifurcation diagram in Fig. 7. It can be seen that the motion of the proposed system behaves atypical chaotic response for $\omega \in [0.15, 1.575]$. On the other hand, for $\omega \in (1.575, 3.1]$, a response of period-one is recorded for the rest of the values of excitation frequency.

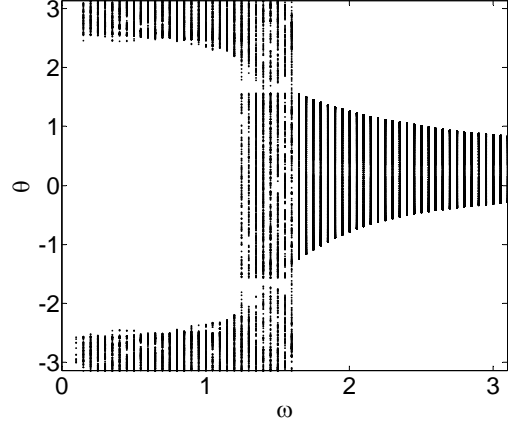
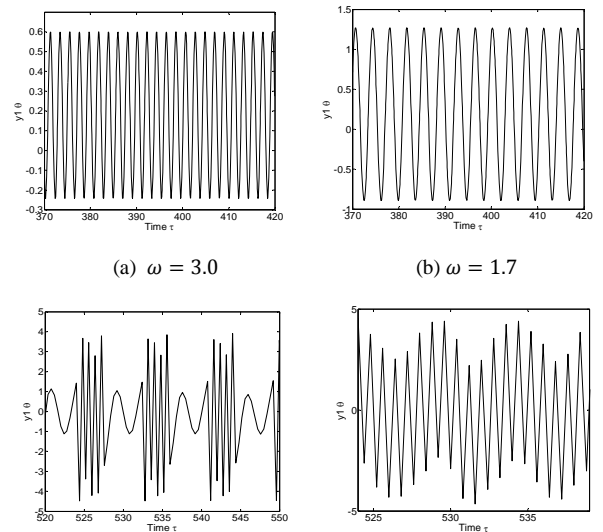


Figure 7. Bifurcation diagram of average progression of the 2-DOF PD system under varying excitation frequency

The numerical investigation also reveals that the characteristic of the irregular transitions, accompanied with the decrease of the values of the branching parameter, behaves atypical responses from periodic to chaotic. These are resulted from the complicated interaction between different coexisting periodic orbits and bifurcations.

The time histories of the angular displacement computed for various frequencies of excitations are presented as well, in which the dynamic behaviors are illustrated. At relatively higher frequency of excitation as shown in Figs. 8 (a) and (b), the pendulum employs simple but steady-state rotations after the initial transients have decayed, which would repeat continuously. On the other hand, the motion contained in Figs. 8 (c) and (d) behaves chaotic response when at relatively lower frequency, which is an extremely complex nonrepeating function of time.



(c) $\omega = 1.5$ (d) $\omega = 1.2$

Figure 8. The time histories of the angular displacement of the inverted pendulum on dimensionless time coordinate

V. SIMULATIONS

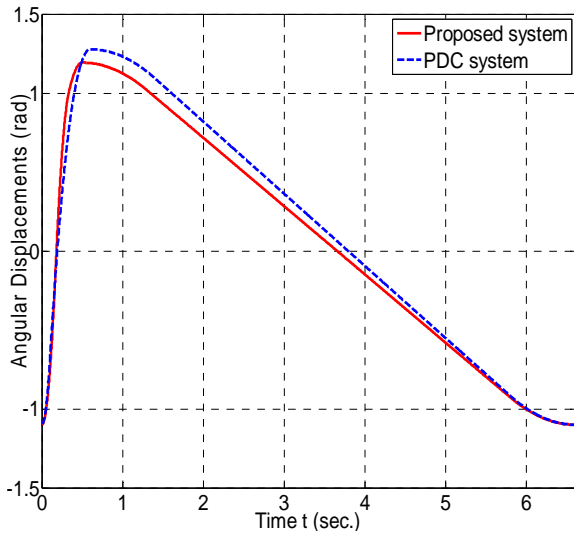
In this section, numerical simulations are presented to verify the effectiveness of the proposed system by employing the closed-loop controller designed in [22]. The performance of the synthesized periodic locomotion principle is also evaluated. The control objective is to make the pendulum track the synthesized locomotion trajectory and simultaneously drive the whole system moving rectilinearly overcoming the environmental resistances.

The numerical simulation results are obtained through MATLAB. The system parameters are selected as $M = 0.5 \text{ kg}$, $m = 0.05 \text{ kg}$, $l = 0.3 \text{ m}$, $g = 9.81 \text{ m/s}^2$, $\mu = 0.01 \text{ N} \cdot \text{m}^{-1}\text{s}^{-1}$, $\rho = 1.8$, $v = 0.6$, $h = 1$, $\omega = 1.7$. The initial conditions are adopted as

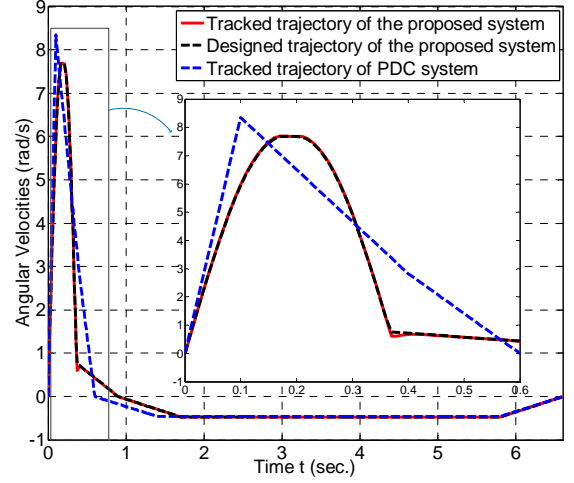
$$\theta(0) = -\theta_0 = -\pi/3, \dot{\theta}(0) = 0, x(0) = 0, \dot{x}(0) = 0 \quad (9)$$

A series of simulations are conducted in comparison to the pendulum-driven cart-pole system proposed in [27], which is referred to as PDC system. Heuristically, the parameter selection approach employed here is trying to find the optimal values such that the best system response is achieved. Note that the numerical investigations in this section are carried out in the un-normalized coordinate.

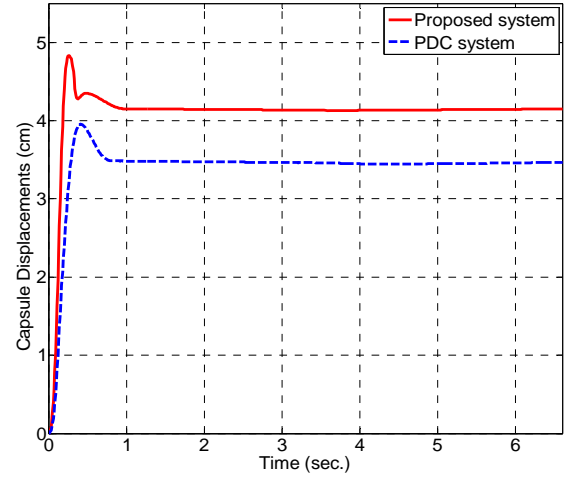
Fig.9 shows the performance comparing results for one cycle in time histories of actuated and passive subsystems, respectively. It is noted that the proposed system periodically actuated under the synthesized locomotion principles behaves steady and intermittent progressive motions. More interestingly, the proposed system and the PDC system travel 4.15cm and 3.5cm, respectively. The trajectories depict in Fig. 9 (b), in particular, show the comparison of tracking performance.



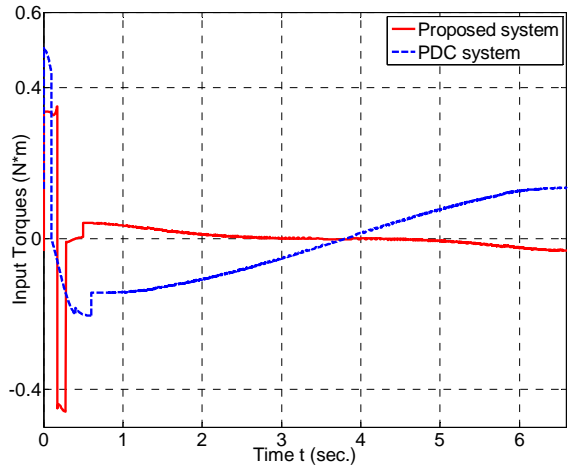
(a) Angular displacement



(b) Trajectory tracking performance



(c) Base displacements

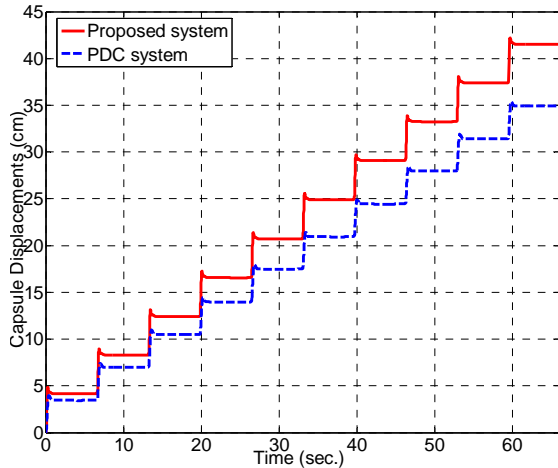


(d) Input torques

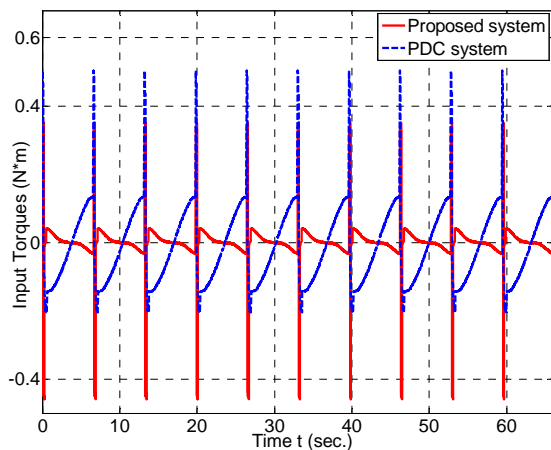
Figure 9. Time histories under closed-loop control for one full cycle

To further evaluate the sequential performance of the proposed system, simulation for ten cycles are conducted as shown in Fig. 10. The proposed system and the PDC system advance 41.5278cm and 34.9335cm, which demonstrate that the PD system has higher efficiencies of 15.88% in progression calculated from Fig. 10 (a). On the other hand, the maximum input torque respectively for

the proposed system and PDC system is $0.4582\text{N}\cdot\text{m}$ and $0.5037\text{N}\cdot\text{m}$. The maximum angular displacement respectively for the proposed system and PDC system are 1.2059rad and 1.2775rad . Therefore the energy consumptions for the proposed system and the PDC system, respectively, are 0.5525J and 0.6435J , which means the proposed system has a 16.46% higher energy efficiency calculated from Fig. 10 (b).



(a) Base displacements



(b) Input torques

Figure 10. Time histories under closed-loop control for ten full cycles

VI. CONCLUSIONS

The issues of periodic locomotion principles synthesis and nonlinear dynamic analysis are studied in this paper. Mathematical models have been established and utilized as a benchmark of numerical analysis to optimize the excitation parameters. The periodic locomotion principles of the actuated subsystem are elaborately studied and synthesized with the characteristic of viscoelastic element. Then the qualitative changes are conducted respectively under the varying excitation amplitude and frequency. Time histories of the pendulum demonstrate a wide variety of system responses, which vary from periodic to chaotic. It is noted that based on the qualitative analysis of the system dynamics, a series of optimal parameters can be obtained, which sheds light on the linkage between nonlinear analysis and trajectory planning for

underactuated locomotion. The simulation results demonstrate the promising performance in more efficient progression and energy consumption.

ACKNOWLEDGMENT

This work is supported by the match funded studentship provided by Bournemouth University and Zhongyuan University of Technology and also supported by the EU Real-time Adaptive networked control of rescue roBOTs (RABOT) project.

REFERENCES

- [1] R. Olfati-Saber, "Nonlinear control of underactuated mechanical systems with application to robotics and aerospace vehicles," Massachusetts Institute of Technology, 2000.
- [2] M. W. Spong, "Underactuated mechanical systems," in *Control problems in robotics and automation*, Springer, 1998, pp. 135–150.
- [3] N. Sun and Y. Fang, "New energy analytical results for the regulation of underactuated overhead cranes: an end-effector motion-based approach," *Ind. Electron. IEEE Trans. On*, vol. 59, no. 12, pp. 4723–4734, 2012.
- [4] Y. Fang, B. Ma, P. Wang, and X. Zhang, "A motion planning-based adaptive control method for an underactuated crane system," *Control Syst. Technol. IEEE Trans. On*, vol. 20, no. 1, pp. 241–248, 2012.
- [5] J. W. Grizzle, G. Abba, and F. Plestan, "Asymptotically stable walking for biped robots: Analysis via systems with impulse effects," *Autom. Control IEEE Trans. On*, vol. 46, no. 1, pp. 51–64, 2001.
- [6] C.-L. Hwang and H.-M. Wu, "Trajectory tracking of a mobile robot with frictions and uncertainties using hierarchical sliding-mode under-actuated control," *IET Control Theory Appl.*, vol. 7, no. 7, pp. 952–965, 2013.
- [7] A. Goswami, B. Espiau, and A. Keramane, "Limit Cycles in a Passive Compass Gait Biped and Passivity-Mimicking Control Laws," *Auton. Robots*, vol. 4, no. 3, pp. 273–286, Sep. 1997.
- [8] X. Xin and T. Yamasaki, "Energy-based swing-up control for a remotely driven Acrobot: Theoretical and experimental results," *Control Syst. Technol. IEEE Trans. On*, vol. 20, no. 4, pp. 1048–1056, 2012.
- [9] R. Jafari, F. B. Mathis, and R. Mukherjee, "Swing-up control of the acrobot: An impulse-momentum approach," in *American Control Conference (ACC), 2011*, 2011, pp. 262–267.
- [10] F. B. Mathis, R. Jafari, and R. Mukherjee, "Impulsive Actuation in Robot Manipulators: Experimental Verification of Pendubot Swing-Up," *Mechatron. IEEEASME Trans. On*, vol. 19, no. 4, pp. 1469–1474, 2014.
- [11] X. Xin, S. Tanaka, J. She, and T. Yamasaki, "New analytical results of energy-based swing-up control for the Pendubot," *Int. J. Non-Linear Mech.*, vol. 52, pp. 110–118, Jun. 2013.
- [12] L. Freidovich, A. Robertsson, A. Shiriaev, and R. Johansson, "Periodic motions of the pendubot via virtual holonomic constraints: Theory and experiments," *Automatica*, vol. 44, no. 3, pp. 785–791, 2008.
- [13] L.-C. Hung and H.-Y. Chung, "Decoupled control using neural network-based sliding-mode controller for nonlinear systems," *Expert Syst. Appl.*, vol. 32, no. 4, pp. 1168–1182, 2007.
- [14] N. Sun, Y. Fang, Y. Zhang, and B. Ma, "A novel kinematic coupling-based trajectory planning method for

- overhead cranes,” *Mechatron. IEEEASME Trans. On*, vol. 17, no. 1, pp. 166–173, 2012.
- [15] Y. Fang, W. E. Dixon, D. M. Dawson, and E. Zergeroglu, “Nonlinear coupling control laws for an underactuated overhead crane system,” *Mechatron. IEEEASME Trans. On*, vol. 8, no. 3, pp. 418–423, 2003.
- [16] L. Freidovich, A. Shiriaev, F. Gordillo, F. Gomez-Esternt, and J. Aracil, “Partial-energy-shaping control for orbital stabilization of high frequency oscillations of the Furuta pendulum,” in *Decision and Control, 2007 46th IEEE Conference on*, 2007, pp. 4637–4642.
- [17] K. J. Aström and K. Furuta, “Swinging up a pendulum by energy control,” *Automatica*, vol. 36, no. 2, pp. 287–295, 2000.
- [18] C. Shi and R. G. Parker, “Modal properties and stability of centrifugal pendulum vibration absorber systems with equally spaced, identical absorbers,” *J. Sound Vib.*, vol. 331, no. 21, pp. 4807–4824, 2012.
- [19] R. Lima, C. Soize, and R. Sampaio, “Robust design optimization with an uncertain model of a nonlinear vibro-impact electro-mechanical system,” *Commun. Nonlinear Sci. Numer. Simul.*, 2014.
- [20] H. Yu, Y. Liu, and T. Yang, “Closed-loop tracking control of a pendulum-driven cart-pole underactuated system,” *Proc. Inst. Mech. Eng. Part J. Syst. Control Eng.*, vol. 222, no. 2, pp. 109–125, 2008.
- [21] H. Yu, T. Yang, Y. Liu, and S. Wane, “A further study of control for a pendulum-driven cart,” *Int. J. Adv. Mechatron. Syst.*, vol. 1, no. 1, p. 44, 2008.
- [22] P. Liu, H. Yu, and S. Cang, “Modelling and control of an elastically joint-actuated cart-pole underactuated system,” in *2014 20th International Conference on Automation and Computing (ICAC)*, 2014, pp. 26–31.
- [23] M. H. Korayem, H. N. Rahimi, and A. Nikoobin, “Mathematical modeling and trajectory planning of mobile manipulators with flexible links and joints,” *Appl. Math. Model.*, vol. 36, no. 7, pp. 3229–3244, 2012.
- [24] E. G. Papadopoulos and D. A. Rey, “A new measure of tipover stability margin for mobile manipulators,” in *Robotics and Automation, 1996. Proceedings., 1996 IEEE International Conference on*, 1996, vol. 4, pp. 3111–3116.
- [25] M. Ruderman, “Modeling of Elastic Robot Joints with Nonlinear Damping and Hysteresis,” in *Robotic Systems - Applications, Control and Programming*, A. Dutta, Ed. InTech, 2012.
- [26] U. Bhattiprolu, P. Davies, and A. K. Bajaj, “Static and Dynamic Response of Beams on Nonlinear Viscoelastic Unilateral Foundations: A Multimode Approach,” *J. Vib. Acoust.*, vol. 136, no. 3, p. 031002, 2014.
- [27] H. Yu, Y. Liu, and T. Yang, “Closed-loop tracking control of a pendulum-driven cart-pole underactuated system,” *Proc. Inst. Mech. Eng. Part J. Syst. Control Eng.*, vol. 222, no. 2, pp. 109–125, 2008.